



Cite this: DOI: 10.1039/d4sc08491h

All publication charges for this article have been paid for by the Royal Society of Chemistry

# Capturing and labeling CO<sub>2</sub> in a jar: mechanochemical <sup>17</sup>O-enrichment and ssNMR study of sodium and potassium (bi)carbonate salts †

Austin Peach,<sup>a</sup> Nicolas Fabregue,<sup>a</sup> Célia Erre,<sup>a</sup> Thomas-Xavier Métro,<sup>a</sup> David Gajan,<sup>b</sup> Frédéric Mentink-Vigier,<sup>c</sup> Faith Scott,<sup>c</sup> Julien Trébosc,<sup>d</sup> Florian Voron,<sup>e</sup> Nicolas Patris,<sup>f</sup> Christel Gervais<sup>g</sup> and Danielle Laurencin<sup>h</sup>

With the rapid increase in temperatures around the planet, the need to develop efficient means to reduce CO<sub>2</sub> emissions has become one of the greatest challenges of the scientific community. Many different strategies are being studied worldwide, one of which consists of trapping the gas in porous materials, either for its short- or long-term capture and storage, or its re-use for the production of value-added compounds. Yet, to further the development of such systems, there is a real need to fully understand their structure and properties, including at the molecular-level following the physisorption and/or chemisorption of CO<sub>2</sub> (which can lead to various species, including carbonate and bicarbonate ions). In this context, <sup>17</sup>O NMR naturally appears as the analytical tool of choice, because of its exquisite sensitivity to probe subtle differences in oxygen bonding environments. To date, it has scarcely been used, due to the very low natural abundance of <sup>17</sup>O (0.04%), and the difficulty in purchasing or obtaining commercial <sup>17</sup>O-labeled compounds adapted to such investigations (e.g., <sup>17</sup>O–CO<sub>2(g)</sub>, or <sup>17</sup>O-enriched Na- and K-(bi)carbonate salts, which can be readily transformed into CO<sub>2</sub>). Herein, we demonstrate how, using mechanochemistry, it is possible to enrich with <sup>17</sup>O a variety of Na- and K-(bi)carbonate salts in a fast, economical, scalable, and user-friendly way. The high enrichment levels enabled recording the first high-resolution <sup>17</sup>O ssNMR spectra of these phases at different temperatures and magnetic fields. From these, the typical spectral signatures of (bi)carbonate ions could be obtained, showing their strong sensitivity to local environments and dynamics. Lastly, we show how thanks to the selective <sup>17</sup>O-labeling, other aspects of the reactivity of carbonates in materials can be unveiled using *in situ* <sup>17</sup>O ssNMR. In the long run, it is expected that this work will open the way to more profound investigations of the structure and properties of carbon capture and storage systems, and, more generally speaking, of functional materials containing carbonates.

Received 16th December 2024

Accepted 20th April 2025

DOI: 10.1039/d4sc08491h

rsc.li/chemical-science

## 1 Introduction

With temperatures constantly rising around the planet, and climate disasters increasing in frequency and intensity, it is

urgent to rapidly develop ways of mitigating the causes of global warming, and notably anthropogenic carbon dioxide (CO<sub>2</sub>) emissions.<sup>1,2</sup> In this context, much research has been dedicated to developing sustainable technologies for substantially reducing the net flow of CO<sub>2</sub> in the atmosphere by capturing it directly at industrial sources, with the aim of storing it either permanently, or temporarily. Several different materials and processes have been investigated for this purpose.<sup>3,4</sup> On one hand, solutions and sorbents involving amine functionalities have been studied for decades, with CO<sub>2</sub> reacting to form ammonium carbamates or (bi)carbonates. However, their toxicity, corrosivity, and/or limited stability and recyclability were demonstrated to be problematic.<sup>5</sup> On the other hand, the potential of mineral carbonation has also been widely studied, including at the industrial scale: it consists of injecting and sequestering CO<sub>2</sub> into “reactive” natural rocks, so that it transforms into carbonate minerals (e.g., calcite and dolomite).<sup>3,6,7</sup> Along the same line, it has been proposed to use

<sup>a</sup>ICGM, Univ. Montpellier, CNRS, ENSCM, Montpellier, France. E-mail: austin.peach@umontpellier.fr; danielle.laurencin@umontpellier.fr

<sup>b</sup>CRMN Lyon, UMR 5082 (CNRS, ENS Lyon, Université Lyon 1), Villeurbanne, France

<sup>c</sup>National High Magnetic Field Laboratory (NHMFL), Florida State University, Tallahassee, Florida, USA

<sup>d</sup>Université de Lille, CNRS, INRAE, Centrale Lille, Université d'Artois FR2638-IMEC-Institut Michel Eugène Chevreul, Lille, France

<sup>e</sup>OSU OREME, UAR 3282, Université de Montpellier, CNRS, IRD, INRAE, Sète, Montpellier, France

<sup>f</sup>HydroSciences Montpellier, UMR 5151, CNRS, IRD, Université de Montpellier, Montpellier, France

<sup>g</sup>LCMCP, UMR 7574, Sorbonne Université, CNRS, Paris, France

† Electronic supplementary information (ESI) available. See DOI: <https://doi.org/10.1039/d4sc08491h>

simple metal oxides like CaO as CO<sub>2</sub> sorbents by formation of CaCO<sub>3</sub>,<sup>8</sup> with applications tested up to the pilot scale. Last but not least, several other classes of materials and sorbents have been investigated for CO<sub>2</sub> capture,<sup>9</sup> including metal organic frameworks (MOFs), which, depending on their structure, can incorporate CO<sub>2</sub> in their pores by physisorption and/or chemisorption.<sup>10–12</sup>

Although a large diversity of systems was studied and developed for CO<sub>2</sub> capture, many aspects of the reactivity of this small molecule still deserve to be studied to ensure the optimal design and understanding of hitherto carbon capture systems. Indeed, beyond the identification of the CO<sub>2</sub> speciation in the final material, which can involve either CO<sub>2</sub> molecules upon physisorption, or (bi)carbonate/carbamate ionic entities upon chemisorption, numerous points are still obscure. Among these, the questions of the impact of temperature, pressure, and moisture on the binding modes of CO<sub>2</sub>, its speciation, and the local molecular motions it undergoes, still need to be investigated in detail, in view of helping conceive and improve, in the long run, the carbon-capture properties of these systems.

As a local analytical probe, NMR spectroscopy naturally appears as perfectly suited for studying CO<sub>2</sub> environments within carbon-capture materials, and it has already been used in numerous investigations.<sup>13–15</sup> To date, the vast majority of NMR studies have concerned carbon-13,<sup>15</sup> due to the higher sensitivity of this spin-1/2 nucleus. Yet, oxygen-17, the only stable isotope of oxygen which can be analyzed by NMR, is also highly attractive:<sup>16</sup> (i) its chemical shift range exceeds 1000 ppm (in comparison to only *ca.* 200 ppm for <sup>13</sup>C); (ii) it is a spin-5/2 quadrupolar nucleus, meaning that complementary information on its local electronic environment can be derived from the quadrupolar parameters  $C_Q$  and  $\eta_Q$  (which is not the case for <sup>13</sup>C, as it is only spin-1/2); (iii) the <sup>17</sup>O lineshape is exquisitely sensitive to molecular-level dynamics, making variable-temperature <sup>17</sup>O NMR studies richly informative on local motions;<sup>17–21</sup> (iv) while only one <sup>13</sup>C resonance is expected per CO<sub>2</sub> molecule or (bi)carbonate/carbamate species attached to a surface, 2 (or 3) distinct <sup>17</sup>O resonances can potentially be observed, meaning that the latter can garner more detailed information on the bonding, reactivity, and adsorption modes of CO<sub>2</sub>.

To the best of our knowledge, <sup>17</sup>O NMR has only been used a small number of times in the context of carbon capture.<sup>14,18,19,22–25</sup> Indeed, the meagre natural abundance of <sup>17</sup>O (0.04%, compared to 1.1% for <sup>13</sup>C) is a real obstacle. In the previous works, only two were performed at natural abundance,<sup>19,23</sup> by using (ultra)-high magnetic fields (*i.e.* 850 MHz to 1.0 GHz NMR instruments), relatively large amounts of sample, and long acquisition times (up to 42 h). However, in these conditions, only 1D NMR spectra could be recorded, which, in the case of ssNMR, hindered the deployment of high-resolution analyses (which are often required to produce robust results). In contrast, when the solid-state NMR investigations were performed on isotopically enriched species, with the initial <sup>17</sup>O-labeling either on the CO<sub>2</sub> gas,<sup>14,19,22</sup> the material of interest,<sup>24</sup> a labeled hydroxide salt,<sup>18</sup> or the surrounding medium (H<sub>2</sub>O),<sup>25</sup> more profound NMR studies were performed, leading to more

extensive information on the structure and reactivity of the systems under investigation. Yet, with limited <sup>17</sup>O-enriched precursors commercially available (the main two being <sup>17</sup>O-enriched water and <sup>17</sup>O–O<sub>2</sub> gas), and limited availability of <sup>17</sup>O-enriched CO<sub>2</sub> gas, any prospect of a widespread application of <sup>17</sup>O ssNMR for the engineering of materials and sorbents for CO<sub>2</sub> capture appears restricted.

Spurred by this general context, we decided to focus on developing efficient and cost-effective routes for enriching in <sup>17</sup>O carbonate and bicarbonate salts of sodium (*i.e.*, Na<sub>2</sub>CO<sub>3</sub>·H<sub>2</sub>O, Na<sub>2</sub>CO<sub>3</sub> and NaHCO<sub>3</sub>), and potassium (*i.e.*, K<sub>2</sub>CO<sub>3</sub>·1.5H<sub>2</sub>O and KHCO<sub>3</sub>). Indeed, three key advantages can be seen in being able to enrich these compounds. First, they are known to decompose upon heat treatment or acidic exposure by releasing CO<sub>2</sub>,<sup>26–29</sup> which makes them attractive sources for the production of <sup>17</sup>O-enriched CO<sub>2</sub>. Second, they encompass a variety of local environments for (bi)carbonate ions, which can be representative of those expected within materials developed for carbon capture. Thus, acquiring high-resolution <sup>17</sup>O ssNMR spectra of these model phases can be seen as a prerequisite for deriving sound conclusions on the structure and dynamics of CO<sub>2</sub>-related species within more complex materials. Last, beyond CO<sub>2</sub>-capture applications, Na- and K-(bi)carbonates are also key precursors for the synthesis of many different types of (bio) materials, meaning that their <sup>17</sup>O enrichment could also be of value for the investigation of a gamut of compounds.

In this manuscript, we first demonstrate how, using mechanochemistry, it is possible to enrich the aforementioned Na- and K-(bi)carbonate salts in <sup>17</sup>O, in a highly efficient way. Then, the high-resolution <sup>17</sup>O ssNMR spectra of the enriched compounds are presented, revealing their strong dependency to the local structure around the (bi)carbonates, and to temperature. Finally, thanks to the high <sup>17</sup>O-enrichment, we show how further aspects of the reactivity of carbonates can be brought to light by *in situ* <sup>17</sup>O ssNMR, which should help propound investigations of the properties of carbon capture materials and/or functional materials containing carbonates.

## 2 Results and discussion

### 2.1 Mechanochemical isotopic enrichment

To the best of our knowledge, two main synthetic approaches have been used so far in the literature for the <sup>17</sup>O-labeling of carbonate salts for ssNMR: (i) the equilibration of carbonate ions in the presence of labeled water (to eventually form enriched Ca- or mixed Ca, Mg-carbonates),<sup>30,31</sup> and (ii) the quantitative reaction of CO<sub>2</sub> gas with pre-labeled LiOH (to form enriched Li<sub>2</sub>CO<sub>3</sub>).<sup>18,32</sup> In the former case, long reaction times (*ca.* 1 week at 90 °C)<sup>30</sup> and/or an excess of expensive <sup>17</sup>O-labeled water were used to ensure sufficient labeling. In the latter case, the synthesis was somewhat constraining, due to the manipulation of *n*-butyllithium in dry THF, and of CO<sub>2</sub> gas at 100 °C.<sup>18,32</sup> From what it appears, these procedures were not optimized in terms of synthetic yields and <sup>17</sup>O-enrichment levels, and their scalability or transposability to other (bi)carbonate salts was not reported. Moreover, these protocols were not widely adopted by other synthetic chemists or spectroscopists, further



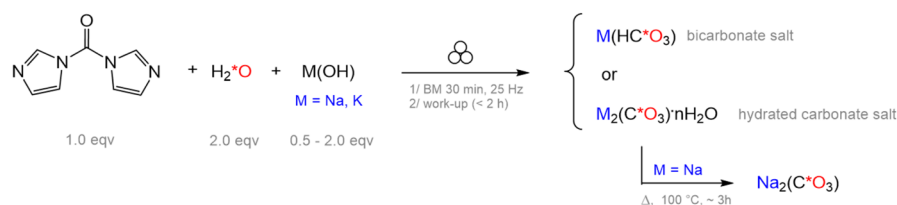
demonstrating the need to develop more efficient enrichment procedures in terms of time, cost, and practicality.

As an alternative, we looked into enriching (bi)carbonate salts by mechanochemistry, using microliter quantities of labeled water ( $\text{H}_2^{18}\text{O}$ ), in a “liquid assisted grinding” type of approach.<sup>33–35</sup> Initial attempts were performed by simply grinding  $\text{Na}_2\text{CO}_3$  in presence of stoichiometric amounts of  $\text{H}_2^{18}\text{O}$ . Indeed, considering that mechanochemical reactions can help accelerate reactions, due to the highly concentrated conditions in the milling jar, we considered the possibility of having a direct isotopic enrichment, by an “equilibration” type of reaction. These first tests were carried out with  $^{18}\text{O}$ -enriched water (which is *ca.* 30-fold cheaper than  $^{17}\text{O}$ -enriched water, when considering their highest enrichments commercially available), and the ball-milling was performed for 30 to 90 minutes, with stainless steel jars and beads. The products recovered after milling were dried and analyzed by powder X-ray diffraction (pXRD) to confirm phase purity, followed by mass-spectrometry (MS) and/or IR spectroscopy to determine if  $^{18}\text{O}$ -labeling had occurred. In the case of IR, no clear isotope-shift was observed, suggesting highly inefficient labeling (if any). Quantitative Isotope-Ratio Mass Spectrometry (IRMS) analyses confirmed that the maximum  $^{18}\text{O}$  level was less than 0.6% (when starting from 99%  $^{18}\text{O}$ -enriched water), which corresponds to a mere 3-fold increase compared to the  $^{18}\text{O}$  natural abundance (0.2%), and remains well beneath the maximum value of *ca.* 40% (calculated for a full scrambling of the oxygen isotopes in the experimental conditions used – see ESI 1†). Although prolonged milling times or increased amounts of labeled water may help further enhance the enrichment level, such experiments were not attempted, as they would decrease the attractiveness of the procedure (*i.e.*, due to the significantly-increased experimental times, cost-prohibitive  $^{17}\text{O}$ -labeling, and/or contaminations from the jar and beads upon longer milling).

A second synthetic approach was thus considered (Fig. 1), which consisted of performing a one-pot quantitative transformation by mechanochemistry. The general idea was to simultaneously introduce in the milling jar *N,N'*-carbonyl-diimidazole (CDI),  $^{17}\text{O}$ -labeled water, and an alkali metal base

(*e.g.*, NaOH or KOH), in order to hydrolyze the CDI precursor to form  $^{17}\text{O}$ -labeled  $\text{CO}_2$ ,<sup>36</sup> and capture this gas with a base to form a (bi)carbonate salt, as  $\text{CO}_2$  is well known to react with bases (whether solvated in aqueous solutions, or present directly in their solid form).<sup>37,38</sup> Initial tests were carried out with non-labeled water (to optimize the synthetic yield), before moving on to  $^{18}\text{O}$ -enriched water (to evaluate the extent of enrichment), and finally  $^{17}\text{O}$ -enriched water (in view of  $^{17}\text{O}$  NMR analyses). The amount of base was adapted to ensure the direct formation of either a bicarbonate or a carbonate salt in the jar. In all cases, full consumption of the NaOH (or KOH) and CDI precursors was observed after only 30 minutes of milling. This was attested by IR spectroscopy (see ESI, Fig. S1–S4†), through (i) the disappearance of the vibration bands characteristic of the reagents (especially the OH stretching band), and (ii) the appearance of the vibration bands of the products (especially the imidazole by-product). The latter was removed during a work-up step, by dissolution in ethanol. The final (bi)carbonate salts were dried, and subsequently characterized by pXRD, IR, and  $^{13}\text{C}$  ssNMR, confirming the formation of phase-pure forms of  $\text{NaHCO}_3$ ,  $\text{KHCO}_3$ ,  $\text{Na}_2\text{CO}_3 \cdot \text{H}_2\text{O}$ , and  $\text{K}_2\text{CO}_3 \cdot 1.5\text{H}_2\text{O}$  (see ESI Fig. S5–S11†). A pure phase of anhydrous  $\text{Na}_2\text{CO}_3$  was isolated by heat-treatment of  $\text{Na}_2\text{CO}_3 \cdot \text{H}_2\text{O}$  for a few hours at 100 °C.

Comparison of the IR spectra of samples prepared using non-labeled,  $^{17}\text{O}$ -labeled, and  $^{18}\text{O}$ -labeled water provided evidence of the successful labeling of the (bi)carbonate salts. This is illustrated in Fig. 2, which highlights some of the spectral regions with variations caused by  $^{17}\text{O}$  or  $^{18}\text{O}$  isotope shifts. Notably, regarding the carbonate salts, the splittings at *ca.* 1065  $\text{cm}^{-1}$  for  $\text{Na}_2\text{CO}_3 \cdot \text{H}_2\text{O}$  and  $\text{K}_2\text{CO}_3 \cdot 1.5\text{H}_2\text{O}$  ( $\nu_1$  stretching mode), and at *ca.* 1775  $\text{cm}^{-1}$  for  $\text{Na}_2\text{CO}_3$  (tentatively assigned to the  $2 \times \nu_2$  harmonic)<sup>42</sup> show contributions from the different  $\text{C}^{16}\text{O}_n \cdot \text{O}_{3-n}^{2-}$  ( $n = 1, 2$  and 3) isotopologues.<sup>43–46</sup> In the case of  $^{18}\text{O}$ -labeled salts, the integration of the relative intensities of these IR bands enabled to estimate the  $^{18}\text{O}$ -enrichment level to be above 25% (when starting from 99%  $^{18}\text{O}$ -labeled water). Analyses of  $^{13}\text{C}$  isotope shifts in solution NMR confirmed this value: for an  $^{18}\text{O}$ -labeled  $\text{Na}_2\text{CO}_3$  phase (prepared from 99%  $^{18}\text{O}$ -labeled water), the  $^{18}\text{O}$ -enrichment level was determined to be *ca.* 30% (see Fig. S12†). IRMS



- ✓ Syntheses achieved within  $\approx 1/2$  day (work-up included)
- ✓ Fully described protocols (with yields and reproducibility tests)
- ✓ Non-hazardous procedures (ambient T and P)
- ✓ Cost-efficient syntheses (stoichiometric amounts of  $^{17}\text{O}$ - $\text{H}_2\text{O}$ )

Fig. 1  $^{17}\text{O}$ -Labeling of Na and K (bi)carbonate salts by mechanochemistry, using a CDI-based procedure.

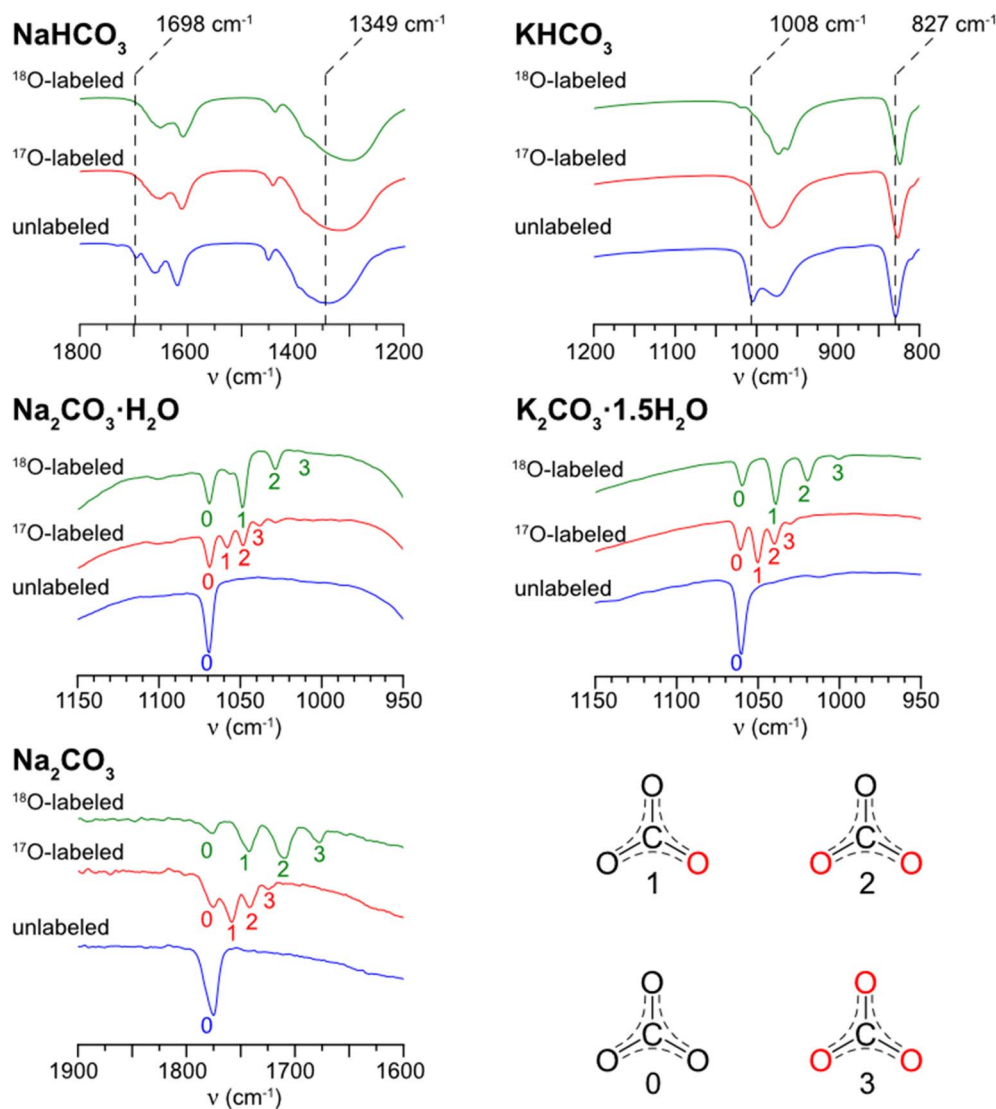


Fig. 2 Experimental IR spectra, zooming into regions of interest for unlabeled (blue),  $^{17}\text{O}$ -labeled (red), and  $^{18}\text{O}$ -labeled (green) Na- and K-(bi) carbonate salts, synthesized by mechanochemistry using the procedure described in Fig. 1. The IR spectra of  $\text{Na}_2\text{CO}_3$ ,  $\text{Na}_2\text{CO}_3 \cdot \text{H}_2\text{O}$ , and  $\text{K}_2\text{CO}_3 \cdot 1.5\text{H}_2\text{O}$  indicate the successful enrichment in  $^{17}\text{O}/^{18}\text{O}$  by the splitting of the IR bands, due to the presence of different isotopologues in the sample (as illustrated in the bottom right corner, in which  $^{17}\text{O}/^{18}\text{O}$ -enriched oxygens are shown in red). The dashed lines in black in the IR spectra of  $\text{NaHCO}_3$  and  $\text{KHCO}_3$  denote IR bands in the unlabeled purified product, which are shifted with respect to those labeled with either  $^{17}\text{O}/^{18}\text{O}$  (assignments of these bands can be found in previous literature).<sup>39–41</sup> The data shown here is for products which were mechanochemically enriched using  $\text{H}_2^{18}\text{O}$  (99%  $^{18}\text{O}$ -labeled), or  $\text{H}_2^{17}\text{O}$  (40%  $^{17}\text{O}$ -labeled for  $\text{Na}_2\text{CO}_3 \cdot \text{H}_2\text{O}$  and  $\text{NaHCO}_3$ , and 90%  $^{17}\text{O}$ -labeled for  $\text{KHCO}_3$  and  $\text{K}_2\text{CO}_3 \cdot 1.5\text{H}_2\text{O}$ ). The  $\text{Na}_2\text{CO}_3$  phase analyzed here was prepared by dehydration of a monohydrate phase, for which labeling had been done by the CDI-based ball-milling procedure, using 70%  $^{17}\text{O}$ -labeled water.

studies on  $^{18}\text{O}$ -labeled Na-carbonates were also performed, further attesting to a significant  $^{18}\text{O}$ -labeling when using the CDI-based protocol (see ESI S1†). Importantly, these measurements imply that an enrichment yield of *ca.* 75% can be achieved with this procedure (see Fig. S12†). Extrapolating to  $^{17}\text{O}$ , this means that when using 70%- $^{17}\text{O}$ -labeled water, an enrichment level of *ca.* 20% can be reached for the (bi)carbonates, which is 500 times more than natural abundance, and amply sufficient for ssNMR analyses, as will be shown below.

Overall, the CDI-based synthesis proposed is particularly efficient for the production of  $^{17}\text{O}/^{18}\text{O}$ -labeled Na- and K-(bi)carbonate salts, enabling to isolate phase-pure compounds in half a day

(work-up included), with a high enrichment level and yield. The protocols are reproducible and user friendly (performed under ambient temperature and pressure), and do not require the use of highly toxic reagents or constraining procedures (*vide supra*). Herein, syntheses are described in quantities enabling the isolation of up to *ca.* 130 mg of product (Table S1†). Yet, experiments can be readily adapted to produce larger amounts of labeled products, by performing reactions simultaneously in two or more jars, increasing the amount of sample per jar, and/or by using larger volume reactors. In the course of our investigations, by simply tripling the initial amount of reagents, we were able to eventually obtain 400 mg of  $^{17}\text{O}$ -enriched  $\text{Na}_2\text{CO}_3$  in just over half





a day, thereby making the CDI-based  $^{17}\text{O}/^{18}\text{O}$ -labeling far more attractive than the previously described carbonate-enrichment schemes.<sup>18,30,32</sup> Although the full details of the enrichment mechanism would deserve further investigation (to rationalize the relative proportions between the isotopologues and the mode of formation of the triply labeled carbonates), at this stage our focus turned to pushing forward  $^{17}\text{O}$  ssNMR studies in view of the study of materials containing (bi)carbonate-related species.

## 2.2 High-resolution $^{17}\text{O}$ ssNMR of $^{17}\text{O}$ -labeled sodium and potassium (bi)carbonates

The  $^{17}\text{O}$  ssNMR spectra of the five Na- and K-(bi)carbonate salts were first acquired at 14.1 T (*i.e.*, 600 MHz instrument) under magic angle spinning (MAS), using standard analytical conditions. For all phases, the successful enrichment enabled the observation of a  $^{17}\text{O}$  NMR signal in just one scan, with some of the spectra shown in Fig. 3A taking as little as 30 minutes (see Table S4† for experimental details). This is a major improvement in comparison to a recently reported work, where the natural abundance spectra of the two K salts (*i.e.*,  $\text{KHCO}_3$  and  $\text{K}_2\text{CO}_3 \cdot 1.5\text{H}_2\text{O}$ ) required more than one day to acquire at higher magnetic field.<sup>19</sup>

$^{17}\text{O}$  NMR signals were observed in two key spectral regions: (i) between 200 and 40 ppm for all Na- and K-(bi)carbonate salts (Fig. 3A, orange zone), which is in the zone expected for carbonate-like environments;<sup>18,19,25,30</sup> and (ii) between 0 and –120 ppm for the two hydrates (Fig. 3A, blue zone), which

corresponds to the zone of crystallographic water.<sup>47–49</sup> The latter signals suggest that some of the excess of enriched water used in the syntheses was incorporated into the hydrated crystal structures. When focussing on the carbonate zone (Fig. 3A, orange), the  $^{17}\text{O}$  NMR spectra appeared either as distorted gaussian lineshapes ( $\text{Na}_2\text{CO}_3 \cdot \text{H}_2\text{O}$  and  $\text{K}_2\text{CO}_3 \cdot 1.5\text{H}_2\text{O}$ ), or as broader asymmetric lineshapes featuring discontinuities typical of second-order quadrupolar central transition (CT) patterns ( $\text{NaHCO}_3$ ,  $\text{KHCO}_3$ , and  $\text{Na}_2\text{CO}_3$ ). Upon closer examination of the spectra of the two bicarbonates, “steps” could be observed on the left part of the signal, indicating an overlap of several  $^{17}\text{O}$  NMR resonances, as expected from the reported crystal structures (which both have 3 crystallographically distinct oxygen environments: 2 C=O and 1 C–OH). Yet, no signature of the C–OH group of the  $\text{HCO}_3^-$  ions was resolved directly by 1D  $^{17}\text{O}$  ssNMR at this magnetic field.

To achieve better resolution in the bicarbonate/carbonate region, the  $^{17}\text{O}$  MAS ssNMR spectra of  $\text{Na}_2\text{CO}_3$ ,  $\text{K}_2\text{CO}_3 \cdot 1.5\text{H}_2\text{O}$ ,  $\text{NaHCO}_3$  and  $\text{KHCO}_3$  (Fig. 3B) were acquired at 28.2 T. Indeed, a significant gain in resolution can be achieved for half-integer quadrupolar nuclei when working at high magnetic fields ( $B_0$ ), since the broadening caused by the second-order quadrupolar interaction is inversely proportional to  $B_0$ .<sup>50</sup> For  $\text{Na}_2\text{CO}_3$  and  $\text{K}_2\text{CO}_3 \cdot 1.5\text{H}_2\text{O}$ , the general appearance of the  $^{17}\text{O}$  NMR lineshapes at 28.2 T remained fairly similar to the one at 14.1 T, albeit much narrower. More importantly, for the bicarbonates, two spectral regions could be resolved (Fig. 3B), which can be assigned to the oxygens belonging to the carbonyl

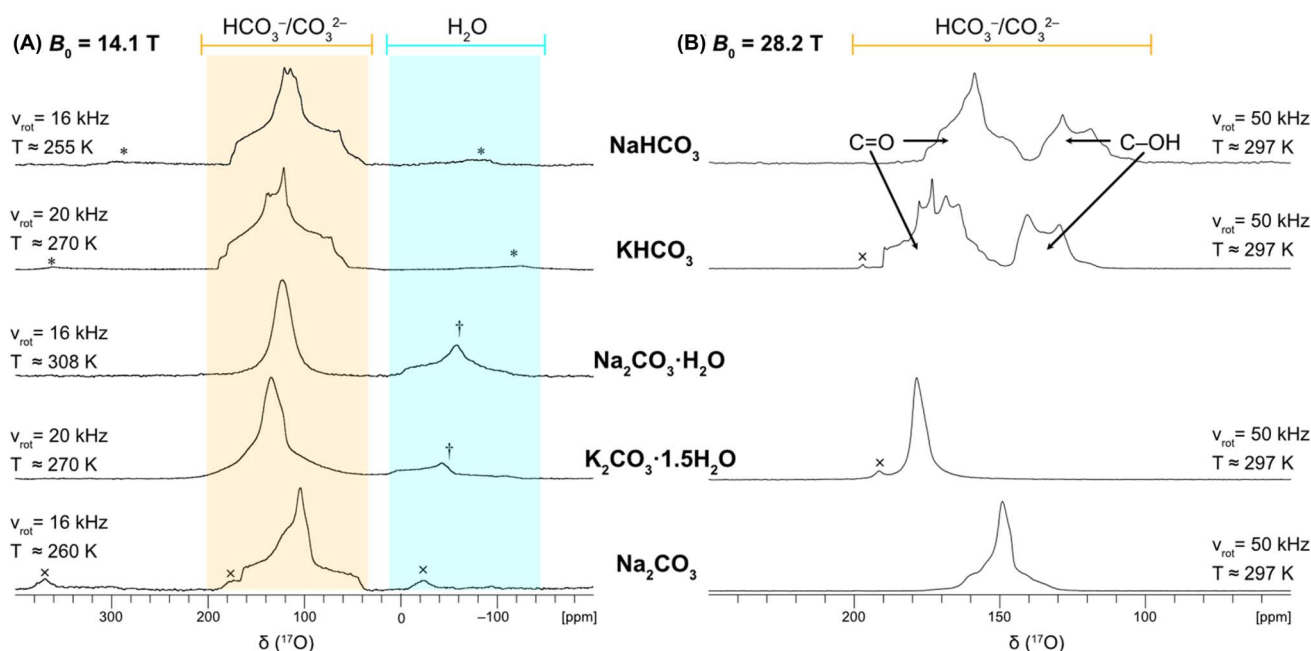


Fig. 3 Experimental  $^{17}\text{O}(^1\text{H})$  MAS NMR spectra acquired at (A)  $B_0 = 14.1$  T (600 MHz instrument) and (B)  $B_0 = 28.2$  T (1.2 GHz instrument) on enriched bicarbonates ( $\text{NaHCO}_3$  and  $\text{KHCO}_3$ ), carbonate hydrates ( $\text{Na}_2\text{CO}_3 \cdot \text{H}_2\text{O}$  and  $\text{K}_2\text{CO}_3 \cdot 1.5\text{H}_2\text{O}$ ), and anhydrous sodium carbonate ( $\text{Na}_2\text{CO}_3$ ). Spinning rates and actual sample temperatures are indicated next to the spectra. In (A), the spectral regions expected for  $\text{HCO}_3^-/\text{CO}_3^{2-}$  (200 to 40 ppm) and crystalline  $\text{H}_2\text{O}$  (0 to –120 ppm) are shown in orange and light blue, respectively. In (B), only the  $\text{HCO}_3^-/\text{CO}_3^{2-}$  spectral region is shown, in which the higher resolution achieved at 28.2 T enables the distinction between C=O and C–OH signals. Spinning sidebands are denoted with an asterisk (\*),  $^{17}\text{O}$  NMR signals arising from crystalline water with a dagger (†), and from satellite transitions with a cross (x). Further details on acquisition parameters are available in the ESI Tables S4 and S5.†



(C=O) and hydroxyl (C–OH) oxygens of  $\text{HCO}_3^-$ . At this stage, we note that the C–OH resonance was not observed in the recently reported natural abundance  $^{17}\text{O}$  NMR spectrum of  $\text{KHCO}_3$ , which may be due to the lack of sensitivity (non-labeled sample) and/or the measurement conditions used (*i.e.* difference in pulse sequence and/or temperature, see Fig. S13†).<sup>19</sup>

In order to extract typical  $^{17}\text{O}$  NMR parameters of bicarbonates (which are needed when interpreting the NMR data of more complex systems), the NMR spectra acquired at 28.2 T were fitted, considering three sites (2 C=O and 1 C–OH, Fig. S14†). Regarding the C=O region (Fig. S14†, green and blue-shaded resonances), the assignment of the resonances was made possible by using 1D and 2D  $^1\text{H}$ – $^{17}\text{O}$  HMQC/INEPT NMR experiments (Fig. S15 and S16†). The NMR parameters were then determined to be as follows, for  $\text{KHCO}_3$  and  $\text{NaHCO}_3$ , respectively (reported in tabulated form in Table S10†):

\*O1 (C=O):  $\delta_{\text{iso}} = 190.6$  and  $175.9$  ppm,  $C_Q = 7.30$  and  $7.21$  MHz, and  $\eta_Q = 0.73$  and  $0.83$ ;

\*O2 (C=O):  $\delta_{\text{iso}} = 178.7$  and  $171.5$  ppm,  $C_Q = 6.75$  and  $6.58$  MHz, and  $\eta_Q = 0.64$  and  $1.00$ ;

\*O3 (C–OH):  $\delta_{\text{iso}} = 146.9$  and  $137.7$  ppm,  $C_Q = 7.30$  and  $7.65$  MHz, and  $\eta_Q = 0.21$  and  $0.39$ .

Here, we note that an early  $^{17}\text{O}$  nuclear quadrupole resonance (NQR) study of  $\text{NaHCO}_3$  and  $\text{KHCO}_3$  at 291 K had reported similar  $C_Q$  and  $\eta_Q$  values for O<sub>2</sub> and O<sub>3</sub>, alongside the same assignment for these sites (see Table S10†).<sup>51</sup> Yet, to the best of our knowledge, it is the first time that experimental values of  $\delta_{\text{iso}}$  for C–OH groups in these bicarbonate salts are reported. Interestingly, the  $\delta_{\text{iso}}$  values for C–OH and C=O groups were all found to be higher for  $\text{KHCO}_3$  than  $\text{NaHCO}_3$ . Such a trend is in line with an early computational study by Wong *et al.* on metal oxalates, where the  $^{17}\text{O}$  isotropic chemical shifts were found to globally increase along the alkali-metal series (*i.e.*,  $\text{Li}^+ < \text{Na}^+ < \text{K}^+ < \text{Rb}^+ < \text{Cs}^+$ ).<sup>52</sup>

Taken together, these  $^{17}\text{O}$  NMR spectra of Na- and K-(bi)carbonate salts demonstrate several significant points. On one hand, the efficient  $^{17}\text{O}$ -labeling using mechanochemistry enabled both improved sensitivity and spectral resolution, allowing the acquisition of high-quality 1D and 2D ssNMR spectra in minutes, and providing direct evidence of the spectral signature of the C–OH group in the bicarbonates. On the other hand, the full spectral assignments of  $\text{KHCO}_3$  and  $\text{NaHCO}_3$  enabled to demonstrate that the range of variation of  $^{17}\text{O}$  NMR parameters for (bi)carbonate anions extends beyond the recently reported values,<sup>19</sup> especially in the case of C–OH groups (Fig. S17†), a point which was further supported by DFT calculations (Table S9†). Such features are highly promising for future studies on more complex (bi)carbonate containing materials by  $^{17}\text{O}$  ssNMR. Despite all the above advantages, only the spectra of the two bicarbonate salts were well resolved at 28.2 T, with the number of distinct  $^{17}\text{O}$  NMR resonances in agreement with the crystal structures. In stark contrast, for  $\text{Na}_2\text{CO}_3 \cdot \text{H}_2\text{O}$  and  $\text{K}_2\text{CO}_3 \cdot 1.5\text{H}_2\text{O}$ , gaussian-like narrow spectra were obtained, suggesting the presence of molecular-level motions around the anions (Fig. 3). Moreover, for anhydrous  $\text{Na}_2\text{CO}_3$ , the two crystallographically inequivalent oxygen sites could not be resolved

under the current measurement conditions, also suggesting the presence of molecular-level dynamics in this material.

To “freeze” these motions,  $^{17}\text{O}$  MAS NMR spectra of the Na- and K-carbonate salts were recorded at 14.1 T under ultra-low temperatures (*i.e.*, sample temperatures *ca.* 105 K) as shown in Fig. S18† (blue spectra). In these conditions, all spectra now appear as well-defined  $^{17}\text{O}$  NMR second-order quadrupolar lineshapes, which is particularly noteworthy for  $\text{Na}_2\text{CO}_3 \cdot \text{H}_2\text{O}$  and  $\text{K}_2\text{CO}_3 \cdot 1.5\text{H}_2\text{O}$ . This highlights that for materials developed for carbon-capture, ultra-low temperature  $^{17}\text{O}$  ssNMR analyses can provide additional means for identifying and resolving the distinct (bi)carbonate local environments. Moreover, it shows that a precise control of the actual sample temperature is needed, to enable robust comparisons of the (bi)carbonate local structure and motions between different samples. Based on these different observations, we then decided to study how  $^{17}\text{O}$  ssNMR may unveil other aspects of carbonate reactivity, in conditions closer to “real-life” application of the materials.

### 2.3 Reactivity of carbonates in the presence of water

In the development of novel systems for carbon capture, the study of the influence of water on the physi- and chemisorption of  $\text{CO}_2$  has been shown to be critical. This holds true not only for purely inorganic sorbents like zeolites and layered double hydroxides,<sup>53,54</sup> but also for porous hybrid materials like MOFs.<sup>55,56</sup> A wide variety of experimental and computational tools have thus been used to investigate the local structure and dynamics around  $\text{H}_2\text{O}$  and  $\text{CO}_2$  (or (bi)carbonate ions), including using  $^{17}\text{O}$  NMR.<sup>19,25</sup> Notably, some studies have shown  $^{17}\text{O}$  isotope exchanges taking place between  $\text{CO}_2$  (or carbonates) and the water present within the interlayer spacings, pores, or at the surface of the material.<sup>14,19,25</sup> Yet, despite that such isotopic exchanges are widely studied in Earth sciences (essentially looking at the  $^{18}\text{O}$  isotopes),<sup>43–45</sup> similar analyses are still underexplored in the investigations on carbon-capture materials. Given that the signatures of water and (bi)carbonates can be distinctly resolved by  $^{17}\text{O}$  NMR, we decided to perform *in situ* NMR analyses on the hydrated carbonates described above, to try to probe isotopic exchange processes between water and (bi)carbonates. More precisely, for the preliminary study described herein, we focused on the monohydrate salt  $\text{Na}_2\text{CO}_3 \cdot \text{H}_2\text{O}$ . Selectively-labeled crystalline  $\text{Na}_2\text{CO}_3 \cdot \text{H}_2\text{O}$  was synthesized by mechanochemistry, with  $^{17}\text{O}$  enrichment on the water only (see ESI S2† for details), to investigate the isotope transfer to the carbonates. The identity and purity of the starting sample were verified by pXRD and IR (Fig. S19†), and the lack of any substantial labeling of the initial carbonate was also confirmed by the latter technique.

*In situ* variable temperature  $^{17}\text{O}$  NMR experiments were recorded on the freshly prepared  $\text{Na}_2\text{CO}_3 \cdot \text{H}_2^{17}\text{O}$  phase (Fig. 4). A broad  $^{17}\text{O}$  NMR signal characteristic of crystalline  $\text{H}_2\text{O}$  was observed between 0 and  $-120$  ppm. No signals were present in the spectral region between 200 and 40 ppm, confirming the absence of any significant (bi)carbonate labeling (Fig. 4B, bottom spectrum). Following this, the sample temperature was increased in increments of 20 K, with spectra recorded at each



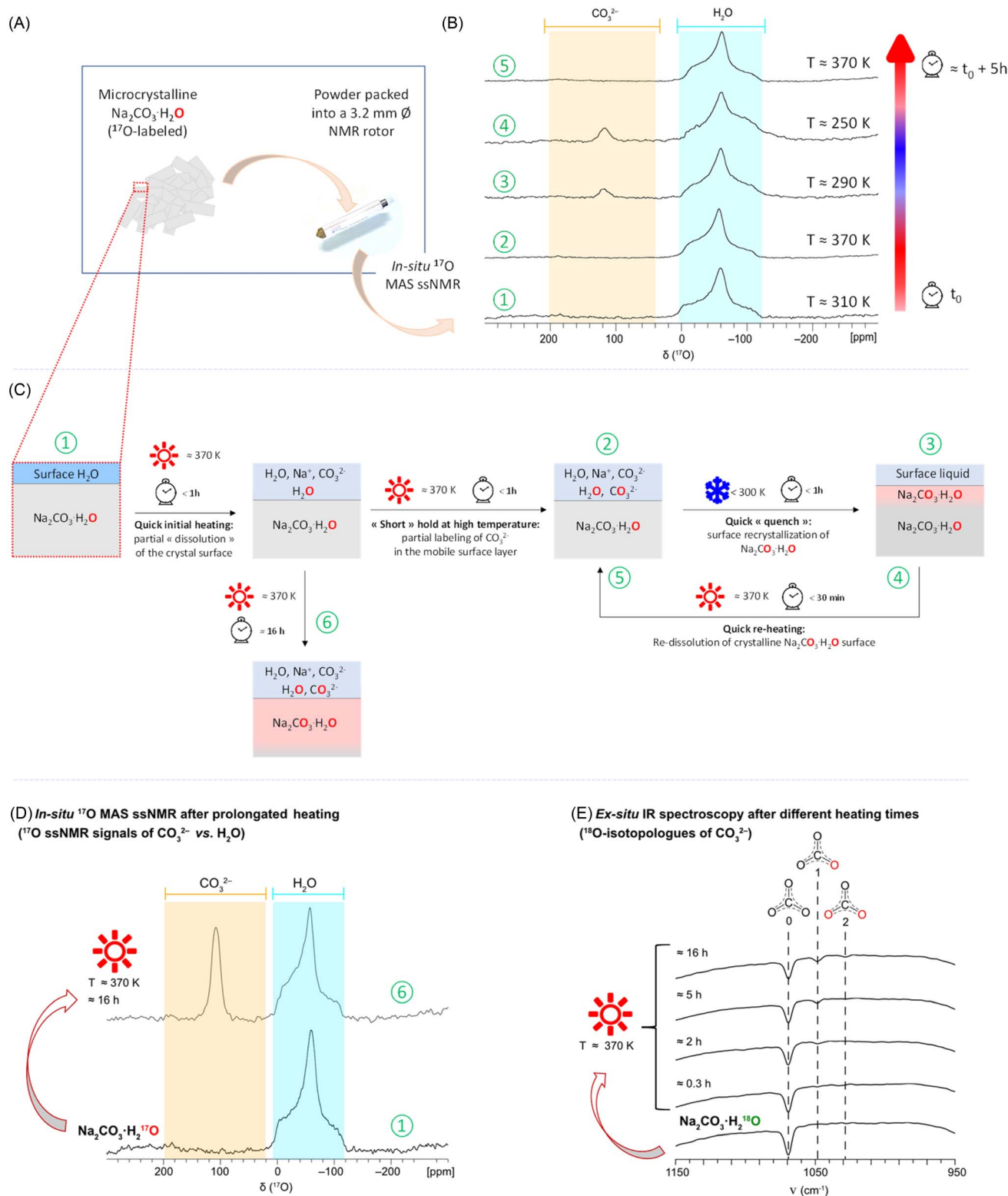


**Fig. 4** (A) Sample environment for the *in situ*  $^{17}\text{O}$  ssNMR study on  $\text{Na}_2\text{CO}_3 \cdot \text{H}_2^{17}\text{O}$  (with initial selective labeling on the water). (B) Experimental VT  $^{17}\text{O}\{^1\text{H}\}$  MAS NMR spectra acquired at  $B_0 = 14.1\text{ T}$  (600 MHz instrument), using the DFS-echo sequence, with sample temperatures indicated on the right for each spectrum. The spectral regions for  $\text{CO}_3^{2-}$  (200 to 40 ppm) and crystalline  $\text{H}_2\text{O}$  (0 to -120 ppm) at this field are shown in orange and light blue, respectively. (C) Schematic representation of the phenomena occurring at the crystal surface accounting for the observations made, with the numbers circled in green referring to the spectra shown in (B) and (D). (D)  $^{17}\text{O}$  ssNMR spectra recorded *in situ* showing that when holding the sample at  $370\text{ K}$  for ca. 16 hours, the carbonate signal is observed, indicating that a substantial amount of labeling has occurred by progressive dissolution/recrystallization of  $\text{Na}_2\text{CO}_3 \cdot \text{H}_2\text{O}$  (see ESI Tables S11 and S12† for further details on acquisition parameters). (E) IR spectra acquired after different time-points on a sample of  $\text{Na}_2\text{CO}_3 \cdot \text{H}_2^{18}\text{O}$  packed into a 3.2 mm rotor and heated in an oven at ca.  $370\text{ K}$ , revealing the progressive increase in labeling of the carbonate overtime (see ESI† 3 for details).

step under identical conditions, up to a maximum sample temperature of 370 K (*ca.* 100 °C). A sub-set of these spectra is shown in Fig. 4, while the full range of  $^{17}\text{O}$  ssNMR experiments are in Fig. S20†. The  $^{17}\text{O}$  NMR spectrum recorded at 370 K was found to be nearly identical to the one initially recorded at *ca.* 310 K. However, when the sample was then “quenched” to *ca.* 290 K, we observed the appearance of a second signal centered around 119 ppm (*i.e.*, in the region characteristic of (bi)carbonates). More specifically, this signal was found precisely at the resonance of the carbonate ions of  $\text{Na}_2\text{CO}_3 \cdot \text{H}_2\text{O}$  at ambient temperature (Fig. S21†). When the sample was then reheated to 370 K, the disappearance of this carbonate peak was observed, and the only signal visible was that of crystalline  $\text{H}_2\text{O}$ . Following these first NMR analyses (performed within a total timeframe of *ca.* 5 hours), the rotor was cooled back down to room temperature and weighed, showing that no significant weight loss had occurred. The sample was unpacked and re-analyzed by pXRD and IR, showing only the distinct fingerprints of the starting monohydrate salt (Fig. S19†).

The  $^{17}\text{O}$  ssNMR spectra shown in Fig. 4B demonstrate that (i) an isotopic exchange between the enriched water and the initially non-labeled carbonates of  $\text{Na}_2\text{CO}_3 \cdot \text{H}_2\text{O}$  has taken place under the experimental conditions used, and (ii)  $^{17}\text{O}$ -labeled carbonate ions may not always be observable in  $^{17}\text{O}$  MAS NMR (as shown here at 370 K), despite their presence in the sample. Complementary analyses were carried out to try to understand these observations, and see how they may be possibly due to the sample preparation and/or measurement conditions. First, when leaving the sample at *ca.* 370 K for a longer period of time (overnight,  $\approx 16$  hours), the  $^{17}\text{O}$  ssNMR spectrum revealed an increase in relative intensity of the signal centered at *ca.* 119 ppm (characteristic of enriched carbonates within the  $\text{Na}_2\text{CO}_3 \cdot \text{H}_2\text{O}$  crystal structure), as shown in Fig. 4D. This demonstrates that the time spent at high temperature allows for a more significant isotope transfer from the labeled water towards the carbonates. This observation was further complemented by IR spectroscopy analyses, by heating up to *ca.* 370 K a freshly prepared  $\text{Na}_2\text{CO}_3 \cdot \text{H}_2^{18}\text{O}$  sample (selectively labeled in  $^{18}\text{O}$  on the water, in order to be able to follow more distinctly the signals of the carbonate isotopologues), and then analyzing it by IR after different periods of time (see ESI S3† for the full experimental details). While no clear enrichment could be detected after only 20 minutes of heating, distinct carbonate vibration bands of the  $^{18}\text{O}$ -labeled isotopologues started to appear after 2 hours, which further increased over time (*e.g.*, after 5 and 16 hours, Fig. 4E). In contrast, when the latter sample was left at lower temperatures overnight (*e.g.* 310 K), no such  $^{18}\text{O}$ -labeling was observed by IR spectroscopy (see Fig. S22†). Second, when analyzing by  $^{17}\text{O}$  NMR the phase which had been heated at *ca.* 370 K overnight, but using other NMR acquisition conditions (*e.g.* direct excitation analyses under MAS or static conditions, instead of an echo), resonances from more mobile  $^{17}\text{O}$ -enriched species became visible, namely  $\text{H}_2\text{O}$  (at *ca.* 0 ppm), and solvated  $\text{CO}_3^{2-}$  ions (at *ca.* 190 ppm)<sup>57</sup> (Fig. S23†). Such resonances were not clearly visible in the initial *in situ* study (spectra shown in Fig. 4B).

From all the above observations, a possible explanation to the appearance/disappearance of the  $\text{Na}_2\text{CO}_3 \cdot \text{H}_2\text{O}$  carbonate signals in Fig. 4B could be the following. Upon the first heating of the sample up to 370 K, a partial surface-dehydration of  $\text{Na}_2\text{CO}_3 \cdot \text{H}_2\text{O}$  takes place, leading to the release of labeled water, which, in the confined environment of the NMR rotor, adds on to the thin water layer already present at the surface of the crystallites, in which the surface  $\text{Na}^+$  and  $\text{CO}_3^{2-}$  ions dissolve. While holding at 370 K, an isotopic exchange process is able to take place in this “liquid-like” layer, leading to the formation of enriched carbonates within a few hours (as shown by IR spectroscopy, Fig. 4E). Because the concentration of these enriched carbonates is initially low (if the sample is only left for less than 30 minutes at 370 K), these are not directly visible at *ca.* 190 ppm in the  $^{17}\text{O}$  MAS NMR spectra obtained at high temperature, when the NMR analyses are performed using an echo type of sequence as in Fig. 4B. However, if the sample is then quenched back to low temperature, the dissolved sodium and carbonate ions recombine to form an enriched  $\text{Na}_2\text{CO}_3 \cdot \text{H}_2\text{O}$  phase at the surface of the initial crystals, with not only  $\text{H}_2\text{O}$  but also a carbonate enrichment now present (signal at 119 ppm). If rapidly heated back up to 370 K, this “enriched” surface layer redissolves, releasing the small amount of labeled  $\text{CO}_3^{2-}$  ions in the liquid-like environment, making them become, again, difficult to detect under analysis conditions shown in Fig. 4B. Though, if the sample is maintained at 370 K overnight, a more significant labeling of the carbonates occurs, with resonances characteristic of enriched “core” carbonate ions (119 ppm) and solvated ones (190 ppm) now detectable by combining Hahn echo and direct-excitation  $^{17}\text{O}$  ssNMR experiments (see Fig. 4D and S23†).

Further investigations would be needed to pinpoint how the isotopic exchange occurs at the molecular scale, and to what extent it depends on the crystallinity and size-distribution of the particles composing the initial powder (as these parameters were found to have a significant effect on the dehydration of  $\text{Na}_2\text{CO}_3 \cdot \text{H}_2\text{O}$ ),<sup>58,59</sup> as well as the sample packing and heating conditions. This would require more extensive analyses, including by variable-temperature  $^{13}\text{C}$  and  $^{23}\text{Na}$  NMR, but also variable-temperature pXRD and electron microscopy, which is beyond the scope of the present work.

Albeit preliminary, this *in situ*  $^{17}\text{O}$  NMR study has several implications. First, it shows that thanks to a selective labeling of the monohydrate, the existence of oxygen-isotopic exchange processes can be revealed, which could become a new handle to study  $\text{CO}_2$  and  $\text{H}_2\text{O}$  interactions/reactivity and compare the properties of different materials developed for carbon capture. Importantly, this investigation clearly highlights the complementarity of *in situ* ssNMR and *ex situ* IR spectroscopy when studying the oxygen isotope-transfer processes, following the  $^{17}\text{O}$  and  $^{18}\text{O}$  isotopes, respectively (as shown in Fig. 4). Second, from a more practical perspective, our present  $^{17}\text{O}$  ssNMR study shows that precaution should be taken in the interpretation of the  $^{17}\text{O}$  MAS NMR spectra recorded for carbonate-containing phases in presence of water. Resonances relative to enriched (bi)carbonate ions may not be visible, depending on sample preparation and/or NMR acquisition conditions chosen (as





shown in Fig. 4B for the 370 K data, and further illustrated in Fig. S13, S23 and S24†). Based on this observation, we would recommend performing analyses at various temperatures (bearing in mind that equilibria can be shifted upon changes in temperature), and with different  $^{17}\text{O}$  ssNMR sequences (e.g. Bloch decay and Hahn echo), in order to avoid missing out on chemical information. Lastly, beyond the study of materials for carbon capture applications, the observation of partial  $^{17}\text{O}$ -isotopic labeling of the carbonates of  $\text{Na}_2\text{CO}_3 \cdot \text{H}_2\text{O}$  at high temperature suggests that it may be possible to directly label hydrated carbonate salts using a “liquid-assisted grinding” approach, while including heating during the milling. With the increasing number of heating set-ups being developed for ball-milling equipment,<sup>60,61</sup> the latter option appears as very valuable to help further expand the scope of carbonate-labeled precursors for other  $^{17}\text{O}$  NMR applications, which we are continuing to develop in our lab.

### 3 Conclusion

In this manuscript, we have described a new strategy for the  $^{17}\text{O}$ -enrichment of Na- and K-(bi)carbonate salts, using mechanochemistry. The synthetic approach is robust, user-friendly, and cost-effective, enabling the production of up to 400 mg of labeled  $\text{Na}_2\text{CO}_3$  in just half a day of manipulation. The high enrichment levels achieved enabled the first high resolution  $^{17}\text{O}$  solid-state NMR analyses to be performed on these materials in short experimental times (as short as 8 minutes for some of the 2D measurements reported here). This enabled carrying out the studies not only at different magnetic fields, but also different temperatures, thereby shedding light on important features regarding the  $^{17}\text{O}$  NMR signatures of (bi)carbonates in solids, among which (i) broad ranges in the variation of the  $^{17}\text{O}$  NMR parameters of C=O and C-OH groups of (bi)carbonates, with notably distinct signatures for the hydroxyl group in  $\text{NaHCO}_3$  and  $\text{KHCO}_3$ ; (ii) a strong sensitivity of their  $^{17}\text{O}$  NMR parameters to temperature (with direct impact on the quadrupolar lineshapes), especially for the hydrated phases, which appeared as “gaussian-like” resonances close to room temperature.

The high  $^{17}\text{O}$ -isotopic labeling achieved on the (bi)carbonate phases was shown to be critical not just to enable accurate spectral fitting, but also to avoid missing out on some resonances at natural abundance, and to help elucidate understudied aspects of the reactivity of (bi)carbonate ions in solids, namely oxygen isotope-transfer processes. As such, the present work provides sound bases for future works on (bi)carbonate-based materials including those developed for  $\text{CO}_2$  capture, for which structure, reactivity, and speciation aspects are key for their rational design. Importantly, we have shown that the  $^{17}\text{O}$  NMR signatures, including during *in situ* investigations, are highly sensitive to temperature and NMR acquisition conditions, meaning that future studies of such materials will require not only an accurate control of the temperature and a careful choice of the pulse sequences, but also analyses at different temperatures, in order to avoid mis-interpretations (or over interpretations) of the data.

Beyond the aforementioned applications, the possibility of labeling with  $^{17}\text{O}$  Na- and K-(bi)carbonate salts opens new avenues to the study of many systems by  $^{17}\text{O}$  ssNMR, as these compounds are widely used as precursors in molecular and materials syntheses, for the preparation of functional (bio)materials, but also organic molecules.<sup>62,63</sup> Moreover, the labeling CDI-based procedure is *a priori* applicable to the enrichment of other metal carbonates (including with transition-metal and lanthanide ions),<sup>64,65</sup> which could then be engaged for the preparation of functional ceramics and glasses, for which  $^{17}\text{O}$  ssNMR is invaluable for establishing structure/property correlations. Last but not least, Na- and K-(bi)carbonates decompose thermally by release of  $\text{CO}_2$ , with a temperature as low as  $\approx 80^\circ\text{C}$  for  $\text{NaHCO}_3$ . These reagents could therefore be used as simple, straightforward, and accessible sources for production of enriched  $\text{CO}_2$ . The latter could then be used for pushing forward investigations on materials for carbon capture using high resolution  $^{17}\text{O}$  NMR. These are points we endeavour to look into, with on-going efforts in our research group.

### Data availability

The data supporting this article have been included as part of the ESI† (i) full description of syntheses, (ii) complementary IR, pXRD, IR-MS, and NMR analyses, including ssNMR acquisition parameters, (iii) computational details; and (iv) a video illustrating the release of  $\text{CO}_2$  during the reaction.

### Author contributions

AP, NF and DL conducted the majority of the research experiments (syntheses, general characterizations and ssNMR analyses). CE contributed to the early stages of the project, by performing the initial syntheses. TXM contributed to the discussion on the mechanochemical syntheses. AP performed the GIPAW-DFT calculations, in close collaboration with CG. CG participated in all discussions regarding computational results. FMV and FS carried out the low-temperature  $^{17}\text{O}$  ssNMR studies at 14.1 T, and DG participated to those at 18.8 T. JT assisted in the ultra-high field ssNMR analyses at 28.2 T. FV and NP performed the MS analyses on the  $^{18}\text{O}$ -labeled compounds. AP and DL wrote the first draft of the manuscript, and all authors contributed to the final preparation of the manuscript.

### Conflicts of interest

There are no conflicts of interest to declare.

### Acknowledgements

This project is funded in part by the European Research Council (ERC) under the European Union's Horizon 2020 research and innovation program (grant agreement no. 772204; 2017 ERC COG, MISOTOP project). Further financial support from the INFRANALYTICS FR2054 for conducting NMR experiments at the CRMN in Lyon and IMEC in Lille is acknowledged. NMR research was also conducted at the National High Magnetic



Field Laboratory (NHMFL, Tallahassee) in Florida, which is supported by the National Science Foundation Cooperative Agreements (No. DMR-2128556), the State of Florida and a partial support by National Institutes of Health Grant (RM1-GM148766 and RM1-GM148556). This project has received support from the European Union's Horizon 2020 research and innovation programme under Grant Agreement 101008500 (PANACEA) and F. J. S. is supported by the postdoctoral scholar award from the Provost's Office at Florida State University. DFT computations were run using high performance computing resources from GENCI-IDRIS (grant no. 2024-AD010815148 and AD10-097535). Philippe Gaveau (ICGM, Montpellier) and Andrew Rankin (IMEC, Lille) are thanked for their experimental expertise and assistance on part of the ssNMR analyses. Dr Jessica Novák-Špačková is warmly acknowledged for early discussions related to this work, Dr Hugo Petitjean for exchanges about the IR data, and Dr Ieva Goldberga for assistance in some initial experiments.

## References

- 1 K. Calvin, D. Dasgupta, G. Krinner, A. Mukherji, P. W. Thorne, C. Trisos, J. Romero, P. Aldunce, K. Barrett, G. Blanco, W. W. L. Cheung, S. Connors, F. Denton, A. Diongue-Niang, D. Dodman, M. Garschagen, O. Geden, B. Hayward, C. Jones, F. Jotzo, T. Krug, R. Lasco, Y.-Y. Lee, V. Masson-Delmotte, M. Meinshausen, K. Mintenbeck, A. Mokssit, F. E. L. Otto, M. Pathak, A. Pirani, E. Poloczanska, H.-O. Pörtner, A. Revi, D. C. Roberts, J. Roy, A. C. Ruane, J. Skea, P. R. Shukla, R. Slade, A. Slangen, Y. Sokona, A. A. Sörensson, M. Tignor, D. van Vuuren, Y.-M. Wei, H. Winkler, P. Zhai, Z. Zommers, J.-C. Hourcade, F. X. Johnson, S. Pachauri, N. P. Simpson, C. Singh, A. Thomas, E. Totin, A. Alegría, K. Armour, B. Bednar-Friedl, K. Blok, G. Cissé, F. Dentener, S. Eriksen, E. Fischer, G. Garner, C. Guivarch, M. Haasnoot, G. Hansen, M. Hauser, E. Hawkins, T. Hermans, R. Kopp, N. Leprince-Ringuet, J. Lewis, D. Ley, C. Ludden, L. Niamir, Z. Nicholls, S. Some, S. Szopa, B. Trewin, K.-I. van der Wijst, G. Winter, M. Witting, A. Birt and M. Ha, *Climate Change 2023: Synthesis Report*, Contribution of Working Groups I, II and III to the Sixth Assessment Report of the Intergovernmental Panel on Climate Change [Core Writing Team], ed. H. Lee and J. Romero, IPCC, Geneva, Switzerland, 2023.
- 2 H. D. Matthews and S. Wynes, *Science*, 2022, **376**, 1404–1409.
- 3 S. Ó. Snæbjörnsdóttir, B. Sigfússon, C. Marieni, D. Goldberg, S. R. Gislason and E. H. Oelkers, *Nat. Rev. Earth Environ.*, 2020, **1**, 90–102.
- 4 B. Dziejarski, J. Serafin, K. Andersson and R. Krzyżyńska, *Mater. Today Sustain.*, 2023, **24**, 100483.
- 5 L. B. Hamdy, C. Goel, J. A. Rudd, A. R. Barron and E. Andreoli, *Mater. Adv.*, 2021, **2**, 5843–5880.
- 6 K. S. Lackner, C. H. Wendt, D. P. Butt, E. L. Joyce and D. H. Sharp, *Energy*, 1995, **20**, 1153–1170.
- 7 H. S. Santos, H. Nguyen, F. Venâncio, D. Ramteke, R. Zevenhoven and P. Kinnunen, *Inorg. Chem. Front.*, 2023, **10**, 2507–2546.
- 8 A. MacKenzie, D. L. Granatstein, E. J. Anthony and J. C. Abanades, *Energy Fuels*, 2007, **21**, 920–926.
- 9 M. E. Zick, D. Cho, J. Ling and P. J. Milner, *ChemNanoMat*, 2023, **9**, e202200436.
- 10 Z. Li, P. Liu, C. Ou and X. Dong, *ACS Sustain. Chem. Eng.*, 2020, **8**, 15378–15404.
- 11 M. Ding, R. W. Flaig, H.-L. Jiang and O. M. Yaghi, *Chem. Soc. Rev.*, 2019, **48**, 2783–2828.
- 12 R. Vismara, S. Terruzzi, A. Maspero, T. Grell, F. Bossola, A. Sironi, S. Galli, J. A. R. Navarro and V. Colombo, *Adv. Mater.*, 2024, **36**, 2209907.
- 13 S. M. Pugh and A. C. Forse, *J. Magn. Reson.*, 2023, **346**, 107343.
- 14 A. H. Berge, S. M. Pugh, M. I. M. M. Short, C. Kaur, Z. Lu, J.-H. Lee, C. J. Pickard, A. Sayari and A. C. Forse, *Nat. Commun.*, 2022, **13**, 7763.
- 15 D. Pereira, R. Fonseca, I. Marin-Montesinos, M. Sardo and L. Mafrá, *Curr. Opin. Colloid Interface Sci.*, 2023, **64**, 101690.
- 16 G. Wu, *Prog. Nucl. Magn. Reson. Spectrosc.*, 2008, **52**, 118–169.
- 17 X. Kong, L. A. O'Dell, V. Tersikh, E. Ye, R. Wang and G. Wu, *J. Am. Chem. Soc.*, 2012, **134**, 14609–14617.
- 18 M. T. Dunstan, J. M. Griffin, F. Blanc, M. Leskes and C. P. Grey, *J. Phys. Chem. C*, 2015, **119**, 24255–24264.
- 19 B. J. Rhodes, L. L. Schaaf, M. E. Zick, S. M. Pugh, J. S. Hilliard, S. Sharma, C. R. Wade, P. J. Milner, G. Csányi and A. C. Forse, *ChemPhysChem*, 2025, **26**, e202400941.
- 20 J. Beerwerth, R. Siegel, L. Hoffmann, L. S. Plaga, M. Storek, B. Bojer, J. Senker, W. Hiller and R. Böhmer, *Appl. Magn. Reson.*, 2020, **51**, 597–620.
- 21 M. Nava, N. Lopez, P. Müller, G. Wu, D. G. Nocera and C. C. Cummins, *J. Am. Chem. Soc.*, 2015, **137**, 14562–14565.
- 22 W. D. Wang, B. E. G. Lucier, V. V. Tersikh, W. Wang and Y. Huang, *J. Phys. Chem. Lett.*, 2014, **5**, 3360–3365.
- 23 M. Y. Hu, X. Deng, K. S. Thanthirawatte, V. E. Jackson, C. Wan, O. Qafoku, D. A. Dixon, A. R. Felmy, K. M. Rosso and J. Z. Hu, *Environ. Sci. Technol.*, 2016, **50**, 12373–12384.
- 24 J.-H. Du, L. Chen, B. Zhang, K. Chen, M. Wang, Y. Wang, I. Hung, Z. Gan, X.-P. Wu, X.-Q. Gong and L. Peng, *Nat. Commun.*, 2022, **13**, 707.
- 25 P. Sahoo, S. Ishihara, K. Yamada, K. Deguchi, S. Ohki, M. Tansho, T. Shimizu, N. Eisaku, R. Sasai, J. Labuta, D. Ishikawa, J. P. Hill, K. Ariga, B. P. Bastakoti, Y. Yamauchi and N. Iyi, *ACS Appl. Mater. Interfaces*, 2014, **6**, 18352–18359.
- 26 D. Paul and G. Skrzypek, *Int. J. Mass Spectrom.*, 2007, **262**, 180–186.
- 27 Y.-L. Wu and S.-M. Shih, *Thermochim. Acta*, 1993, **223**, 177–186.
- 28 M. Hartman, K. Svoboda, B. Čech, M. Pohořelý and M. Šyc, *Ind. Eng. Chem. Res.*, 2019, **58**, 2868–2881.
- 29 J. M. McCrea, *J. Chem. Phys.*, 1950, **18**, 849–857.
- 30 M. E. Smith, S. Steuernagel and H. J. Whitfield, *Solid State Nucl. Magn. Reson.*, 1995, **4**, 313–316.
- 31 J. Ihli, J. N. Clark, N. Kanwal, Y.-Y. Kim, M. A. Holden, R. J. Harder, C. C. Tang, S. E. Ashbrook, I. K. Robinson and F. C. Meldrum, *Chem. Sci.*, 2019, **10**, 1176–1185.



- 32 M. Leskes, A. J. Moore, G. R. Goward and C. P. Grey, *J. Phys. Chem. C*, 2013, **117**, 26929–26939.
- 33 T.-X. Métro, C. Gervais, A. Martinez, C. Bonhomme and D. Laurencin, *Angew. Chem., Int. Ed.*, 2017, **56**, 6803–6807.
- 34 C.-H. Chen, E. Gaillard, F. Mentink-Vigier, K. Chen, Z. Gan, P. Gaveau, B. Rebière, R. Berthelot, P. Florian, C. Bonhomme, M. E. Smith, T.-X. Métro, B. Alonso and D. Laurencin, *Inorg. Chem.*, 2020, **59**, 13050–13066.
- 35 J. Špačková, I. Goldberga, R. Yadav, G. Cazals, A. Lebrun, P. Verdié, T. Métro and D. Laurencin, *Chem.–Eur. J.*, 2023, **29**, e202203014.
- 36 K. M. Engstrom, A. Sheikh, R. Ho and R. W. Miller, *Org. Process Res. Dev.*, 2014, **18**, 488–494.
- 37 L. Rincón, C. Ruiz, R. R. Contreras and J. Almarza, *Environ. Sci.:Adv.*, 2023, **2**, 957–966.
- 38 M. Yoo, S. J. Han and J. H. Wee, *J. Environ. Manag.*, 2013, **114**, 512–519.
- 39 A. Novak, P. Saumagne and L. Bok, *J. Chim. Phys.*, 1963, **60**, 1385–1395.
- 40 A. Bertoluzza, P. Monti, M. A. Morelli and M. A. Battaglia, *J. Mol. Struct.*, 1981, **73**, 19–29.
- 41 G. Lucazeau and A. Novak, *J. Raman Spectrosc.*, 1973, **1**, 573–586.
- 42 W. W. Rudolph, G. Irmer and E. Königsberger, *Dalton Trans.*, 2008, 900–908.
- 43 T. Geisler, C. Perdikouri, A. Kasiotas and M. Dietzel, *Geochim. Cosmochim. Acta*, 2012, **90**, 1–11.
- 44 A. Landuyt, P. V. Kumar, J. A. Yuwono, A. H. Bork, F. Donat, P. M. Abdala and C. R. Müller, *JACS Au*, 2022, **2**, 2731–2741.
- 45 S. Wang, K. Lu, T. Wang, J. Wu, H. Zheng and Y. Huang, *Spectrochim. Acta, Part A*, 2020, **241**, 118648.
- 46 Q. Wu, N. Yang, M. Xiao, W. Wang and C. Cui, *Nat. Commun.*, 2024, **15**, 9145.
- 47 S. Nour, C. M. Widdifield, L. Kobera, K. M. N. Burgess, D. Errulat, V. V. Tersikh and D. L. Bryce, *Can. J. Chem.*, 2016, **94**, 189–197.
- 48 I. Goldberga, N. Patris, C.-H. Chen, E. Thomassot, J. Trébosc, I. Hung, Z. Gan, D. Berthomieu, T.-X. Métro, C. Bonhomme, C. Gervais and D. Laurencin, *J. Phys. Chem. C*, 2022, **126**, 12044–12059.
- 49 E. G. Keeler, V. K. Michaelis, C. B. Wilson, I. Hung, X. Wang, Z. Gan and R. G. Griffin, *J. Phys. Chem. B*, 2019, **123**, 3061–3067.
- 50 R. E. Wasylshen, S. E. Ashbrook and S. Wimperis, *NMR of Quadrupolar Nuclei in Solid Materials*, John Wiley & Sons Ltd, 2012.
- 51 I. J. F. Poplett and J. A. S. Smith, *J. Chem. Soc., Faraday Trans. 2*, 1981, **77**, 761–796.
- 52 A. Wong, G. Thurgood, R. Dupree and M. E. Smith, *Chem. Phys.*, 2007, **337**, 144–150.
- 53 D. G. Boer, J. Langerak and P. P. Pescarmona, *ACS Appl. Energy Mater.*, 2023, **6**, 2634–2656.
- 54 L. Santamaría, S. A. Korili and A. Gil, *Chem. Eng. J.*, 2023, **455**, 140551.
- 55 I. Erucar and S. Keskin, *Ind. Eng. Chem. Res.*, 2020, **59**, 3141–3152.
- 56 A. Rajendran, G. K. H. Shimizu and T. K. Woo, *Adv. Mater.*, 2024, **36**, 2301730.
- 57 B. N. Figgis, R. G. Kidd and R. S. Nyholm, *Proc. R. Soc. London, Ser. A*, 1962, **269**, 469–480.
- 58 S. Fukunaga, Y. Zushi, M. Hotta and N. Koga, *Phys. Chem. Chem. Phys.*, 2025, **27**, 3384–3400.
- 59 Y. Zushi, S. Iwasaki and N. Koga, *Phys. Chem. Chem. Phys.*, 2022, **24**, 15736–15748.
- 60 G. Félix, N. Fabregue, C. Leroy, T. X. Métro, C. H. Chen and D. Laurencin, *Phys. Chem. Chem. Phys.*, 2023, **25**, 23435–23447.
- 61 N. Cindro, M. Tireli, B. Karadeniz, T. Mrla and K. Užarević, *ACS Sustain. Chem. Eng.*, 2019, **7**, 16301–16309.
- 62 F. Mele, A. Aquilini, A. M. Constantin, F. Pancrazzi, L. Righi, A. Porcheddu, R. Maggi, D. A. Cauzzi, G. Maestri, E. Motti, L. Capaldo and N. Della Ca', *ChemRxiv*, 2025, preprint, DOI: [10.26434/chemrxiv-2024-zm9fw-v3](https://doi.org/10.26434/chemrxiv-2024-zm9fw-v3).
- 63 M. Sander, S. Fabig and L. Borchardt, *Chem.–Eur. J.*, 2023, **29**, e202202860.
- 64 P. Vishnu Vardhan, C. Jothilakshmi, U. Kamachi Mudali and S. Devaraj, *Mater. Today: Proc.*, 2017, **4**, 12407–12415.
- 65 P. Barai, X. Wang, M. Wolfman, J. Chen, A. Gutierrez, J. C. Garcia, J. Wen, T. Kinnibrugh, T. T. Fister, H. H. Iddir and V. Srinivasan, *J. Mater. Chem. A*, 2024, **12**, 12835–12855.

